Rigid magnetic foam-like behavior in ball-milled FeAl

L. F. Kiss, D. Kaptás, J. Balogh, L. Bujdosó, T. Kemény, and L. Vincze
Research Institute for Solid State Physics and Optics, H-1525 Budapest P.O.Box 49, Hungary

J. Gubicza
Solid State Physics Department, Eötvös University, Budapest, Hungary
(Received 20 April 2004; published 28 July 2004)

After ball-milling nonmagnetic FeAl a grain structure resembling to a rigid magnetic foam is indicated by Mössbauer spectroscopy. It consists of nanosize nonmagnetic grains with ferromagnetic boundaries formed by about two atomic layers of Fe. The magnetic behavior is uncommon: (i) the transition to the paramagnetic state is *glass-like* and magnetic relaxation sets in at low temperatures; (ii) the *magnitude* of the local Fe magnetic moments decreases *linearly* with temperature; (iii) in high fields a *strongly anisotropic* ferromagnetic behavior is observed.

DOI: 10.1103/PhysRevB.70.012408 PACS number(s): 75.50.Tt, 75.75+a, 76.80.+y, 81.20.Ev

Many studies have already made evident that the magnetic properties of nanosize objects are to a large extent determined by the surface properties.[1,2] Surface atoms may have magnetic anisotropies, moments, and even magnetic ordering significantly different from those of the bulk atoms due to their altered topological arrangement, reduced coordination, and increased volume. Despite this, separation of the surface effects from other special features of the nanomaterials is far from trivial. In most sample preparation techniques (evaporation, ball milling, chemical reduction, etc.[3]) both the surface and the bulk properties are influenced by impurities, mixing, and disordering of the components. A definitive scaling with the inverse characteristic length of the nanosize objects is rarely observed. A magnetic foam without substrate, i.e., a nonmagnetic volume (bubble) surrounded by a continuous magnetic layer, would exhibit solely surface and/or thin film effects. Former studies of magnetic foams concentrated[4] mostly on the field dependence of the coarsening of the domain patterns of fluid froths. We are not aware of any study of the fundamental magnetic properties of a frozen foam. In the following it will be shown that ball-milled FeAl is a good candidate for the material that can be termed as a rigid magnetic foam.

The structure of Fe-Al alloys is based on the bcc lattice of α-Fe in a broad concentration range.[5] Two ordered phases appear around the stoichiometric FeAl and Fe_3Al. FeAl crystallizes to a CsCl-type (B2) crystal structure, in which each Fe atom has 8 Al nearest and 6 Fe next nearest neighbors. Ordered Fe_3Al has $D0_3$-type structure, where the Fe I atoms have 8 Fe nearest and 6 Al next nearest neighbors, while the atoms of the pure Fe sublattice (Fe II) are surrounded by 4 Fe I and 4 Al (forming a tetrahedron) first neighbors, and 6 Fe II next nearest neighbors. FeAl is nonmagnetic, and the bcc Fe-Al solid solution and Fe_3Al are ferromagnetic. Ferromagnetism rapidly transforms into a complex magnetic state between 30 and 50 at.% Al content. It is often described[6] as a spin-glass state following the hypothesis of Sato and Arrott[7] on antiferromagnetic Fe-Al-Fe superexchange. Cold-working restores[8,9] ferromagnetism due to the formation of antiphase boundaries (APB's) and due to the effects of the local environments on the magnetic state of a given Fe atom. The magnitude of the iron magnetic moments depends[10] on the number of iron nearest neighbors: it is about the same as in pure α-Fe($2.2\mu_B$) for five or more nearest Fe neighbors, and the iron atoms having less than four Fe nearest neighbors are nonmagnetic. The concentration dependence of the average magnetization yields $1.8\mu_B$ for the magnetic moment of Fe atoms with a 4 Fe−4 Al first neighbor environment, which is slightly larger than the room-temperature value measured[11] by neutron diffraction in Fe_3Al [$\mu_{\mathrm{Fe\ II}} = (1.50 \pm 0.10)\mu_B$]. In the stoichiometric ordered B2 structure APB (i.e., the partial replacement of an Al plane by an Fe plane) creates magnetic moments on the formerly nonmagnetic iron atoms since the number of the nearest Fe neighbors reaches 4 Fe along the boundary. Off-stoichiometry amplifies[12] this effect drastically.

The stoichiometric FeAl ingot was prepared by induction melting in a cold crucible. X-ray diffraction and low-temperature Mössbauer measurement confirmed the well-ordered B2 state. Mechanical milling was carried out in a vibrating frame hardened steel single ball vessel,[3,13] which was continuously evacuated by a turbomolecular pump system. Annealing of the powders at 650−700 K restored the well-ordered B2 state and no composition change or contamination was detected by Mössbauer measurements.

The x-ray diffractograms were measured by a Philips X'pert powder diffractometer using Cu K_α radiation. The grain size of the granules, D, was determined from the full width at half maximum of the x-ray diffraction profiles by the modified Williamson-Hall procedure[14] as 21 ± 2, 13 ± 2, and 8 ± 1 nm after 1, 10, and 100 h of ball-milling, respectively.

^{57}Fe Mössbauer spectra were recorded by a constant acceleration spectrometer between 4.2 and 300 K, and in external magnetic fields using a 7 T Janis superconducting magnet. Standard procedures were used for the evaluation of the spectra: the ordered B2 component is fitted with a single Lorentzian line and after subtracting this curve from the measured spectra, the remaining part was described by binomial distributions.[15] The magnetization measurements were

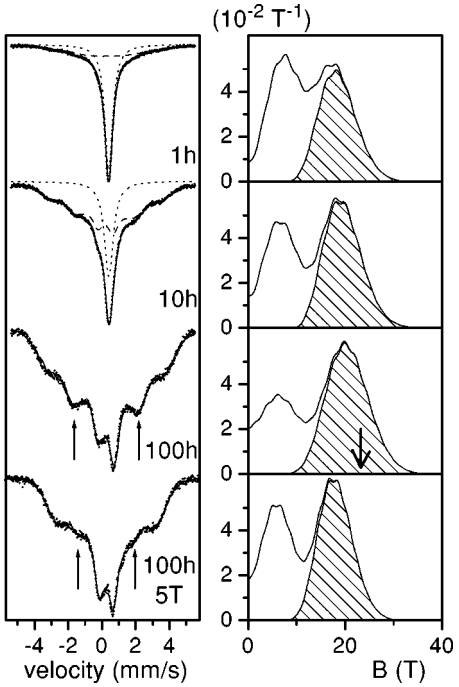

FIG. 1. 4.2 K Mössbauer spectra of FeAl ball-milled for different times. Full, broken, and dotted lines are fitted curves of the full spectra and the magnetic and the paramagnetic components, respectively. In the hyperfine field distributions fitted to the magnetic components shading and an arrow marks the hyperfine field of Fe atoms with localized moments and that of Fe atoms with 4 Al–4 Fe nearest neighbors in Fe_3Al (Ref. 19), respectively. The positions of the second and fifth lines for the high field peak in the spectra of the 100 h sample in 0 T and 5 T field are marked as well.

performed by a Quantum Design MPMS-5S SQUID magnetometer with a maximum field of 5 T.

Ball-milling of the FeAl ingot leads to the gradual disordering of the ordered B2 structure as shown by the Mössbauer spectra in Fig. 1. The single line corresponding to the ordered nonmagnetic phase disappears for the 100 h ball-milled sample but the crystal structure remains bcc with an increase in the lattice parameter (from 0.2906 to 0.2927 nm). Parallel to this process an increasing amount of broad, magnetic component appears that has a double-peaked hyperfine field (hf) distribution. Fe hyperfine fields with similar structure were observed[16] in off-stoichiometric ordered Fe-Al alloys and the large hyperfine fields were attributed to Fe atoms with magnetic moments. In Fe-Al alloys with bcc structure the iron hyperfine fields and magnetic moments are not directly proportional. The nonlocalized contribution of the iron hf (i.e., conduction electron polarization by the neighboring magnetic iron atoms) exceeds 50% in the bcc solid solution.[17] This transferred contribution is proportional to the magnetic moment of the individual neighbors, the proportionality coefficients may differ[18] for the $D0_3$ and the B2 structure. Consequently the nonmagnetic Fe atoms also experience hyperfine fields though substantially smaller than the magnetic Fe atoms, and the low-field part of the hf distribution in Fig. 1 is to be attributed to the nonmagnetic Fe atoms with magnetic neighbors.

The magnetic iron atoms mostly belong to the grain boundaries in the ball-milled samples. Their percentage p_M is

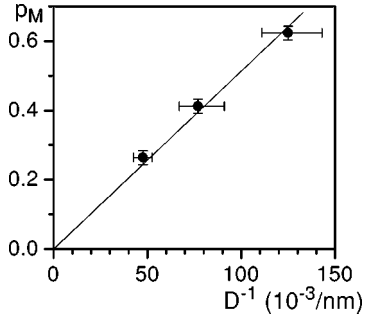

FIG. 2. The fraction of magnetic Fe atoms, p_M, in the ball-milled FeAl alloys as a function of the inverse grain size, D^{-1}. The proportionality is shown by the full line.

determined as the spectral weight belonging to the high-field part of the hf distribution marked by shadowing in Fig. 1. p_M correlates well with the inverse of the average grain size (Fig. 2). The slope of this correlation is proportional to the thickness of the boundary region, d. The proportionality coefficient is dependent on the shape of the grains; in the simplest cases (sphere or cube) it is $6d$. In our case this relation gives $d \approx 0.8$ nm for the average thickness of the grain boundaries. It may be somewhat overestimated due to the well-known bias of x-ray diffraction by the contribution of larger grains and to some disorder within the grains.

The average hf of the high-field part of the distribution, B_m, is attributed to Fe atoms with 4 Fe and 4 Al nearest neighbors. It is somewhat lower than the hf of Fe II in Fe_3Al (23.4 T, extrapolated from the room-temperature value[19]) in line with a smaller delocalized contribution. In Fe_3Al the neighbors of Fe II atoms have 8 Fe neighbors (Fe I) and larger magnetic moments, while in the ball-milled samples the number of Fe environments with 5 or more Fe nearest neighbors is small. (In a completely disordered FeAl alloy this contribution would be around 36%.) In the ball-milled alloys the hf of the Fe I sites of Fe_3Al with 8 Fe neighbors [32.6 T (Ref. 19)] is not present and B_m is slightly increasing with increasing amount of the magnetic Fe atoms (i.e., with milling time). As a consequence the average iron moment is increasing since more formerly nonmagnetic atoms will have magnetic moments, which supports the above assignment. The simplest explanation is the formation of antiphase grain boundaries. If two bcc iron layers are surrounded on both sides by Al layers, then each Fe atom will have 4 Fe–4 Al nearest neighbor environments. The absence of a single line in the Mössbauer spectrum of the 100 h ball-milled sample indicates the disordering of the B2 structure for ball milling.

Figure 3 shows the results of the SQUID measurements. In small magnetic fields the magnetization shows a broad peak as a function of temperature both in field- and in zero-field-cooled states. The thermomagnetic curve for the 1 h ball-milled sample not shown is similar but on a smaller scale to that of the 10 h ball-milled one. This feature resembles the freezing of a spin glass. However, the zero-field Mössbauer measurements (Fig. 4) show no magnetic character around the temperature of the peaks. Indeed, the Mössbauer spectra show no well-defined transition from the magnetic to the nonmagnetic state: superparamagnetic relaxation

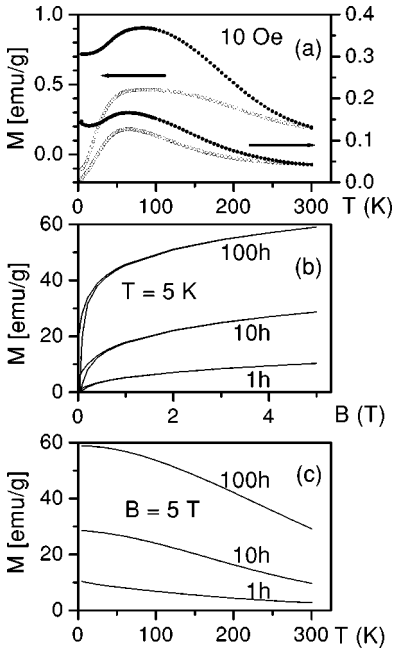

FIG. 3. Low-field behavior of the 10 h (right) and 100 h (left) ball-milled FeAl alloys in zero-field (circles) and in field-cooled (dots) states (a), the magnetization as a function of external field at 5 K (b), and temperature dependence in 5 T external field (c).

starts already at 12 K and 50 K for the 1 h and 100 h ball-milled samples, respectively. It means that already small magnetic fields influence greatly the magnetic state of these alloys. However, the magnetization cannot be saturated even in 5 T (Fig. 3(b)), which is expected for spin glasses with antiferromagnetically coupled magnetic moments. The thermomagnetic curves in 5 T show complex temperature dependences and no distinct features (Fig. 3(c)). In contrast, the magnitude of B_m, i.e., that of the Fe magnetic moment decreases linearly with temperature (Fig. 5). This linear decrease is not well understood,[2] and superparamagnetic relaxation might be a possible explanation.

Ferromagnetic but highly anisotropic behavior is shown by the Mössbauer spectra in applied magnetic fields. Information on the direction of the Fe magnetic moments is given by the relative intensity of the second and fifth lines, $I_{2,5}$, of the spectra (corresponding to the $\Delta m=0$ nuclear transitions). $I_{2,5}=4\sin^2\theta/(1+\cos^2\theta)$, where θ is the angle between the magnetic moment and the magnetic field B_{ext} applied parallel to the γ-beam direction. $I_{2,5}=2$ found without applied field (Fig. 1) corresponds to a random Fe spin orientation. For complete saturation, i.e., when all the magnetic moments are collinear to B_{ext}, $I_{2,5}=0$. Despite that this state was not reached at 4.2 K even in 7 T (our highest available external field), $I_{2,5}$ continuously decreased for increasing B_{ext}, signaling the gradual alignment of the canted magnetic moments. If a linear extrapolation is justified, at least 14 T and 18 T would be necessary to reach saturation for the 100 h and 10 h ball-milled samples, respectively. Similar strong magnetic anisotropy is reported[9] for ferromagnetic clusters along the APB in off-stoichiometric Fe-Al alloys.

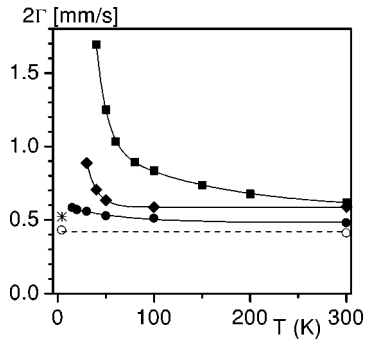

FIG. 4. Full width at half maximum (2Γ) of the paramagnetic line in the Mössbauer spectra as a function of temperature for 100 h (squares), 10 h (diamonds), and 1 h (full circles) ball-milled FeAl samples, respectively. Star and empty circles mark the values for the as-received sample and for the 100 h ball-milled one annealed at 720 K, respectively. Continuous and broken lines are guides to the eye.

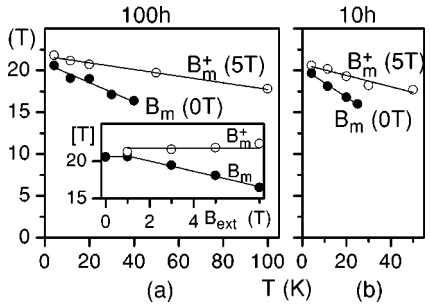

FIG. 5. Temperature dependence of the hf of the localized Fe magnetic moments in 0 T (B_m, dots) and in 5 T (B_m^+, circles) for the 100 h (a) and 10 h (b) ball-milled FeAl, respectively. The inset shows the external field dependence of B_m (dots) at 4.2 K; it is corrected for the applied field and the canting angle as explained in the text (B_m^+, circles).

The hf is oriented antiparallel to the magnetic moment. In the collinear ferromagnetic state the absolute value of the hf should decrease with the value of the applied field when it is larger than the demagnetizing field. In the case of a canted moment the decrease is $B_{ext}\cos\theta$. Obviously, the hf of antiferromagnetically coupled moments should increase with this amount. Thus the increase of the standard width of the distribution around B_m should occur if magnetic moments with random directions were present as in a spin glass. Experimentally a decreasing width with increasing B_{ext} was found, which is expected for a strong random anisotropy dominated ferromagnet. (For the example shown in Fig. 1 the standard width of the distribution around B_m decreases from 4.2 T to 3.4 T by applying 5 T.) In the case of ferromagnetic coupling the applied field results in the decrease of B_m, as well. If it is compensated, i.e., $B_m^+=B_m+B_{ext}\cos\theta$ is plotted vs B_{ext}, a saturation with zero slope is expected. The inset of Fig. 5 shows that this expectation is well fulfilled (the value of $\cos\theta$ is determined from the measured $I_{2,5}$ intensities). B_m^+ is a measure of the iron magnetic moments in the applied field and it also decreases linearly with the temperature like B_m (Fig. 5).

The value of the average iron magnetic moment, $\overline{\mu}_{\mathrm{Fe}}$, obtained in the magnetization measurement is related to the p_M number, the μ_{Fe} moment of the magnetic iron atoms, and the

θ angle between the magnetic moment and applied field as $\overline{\mu}_{\mathrm{Fe}}=\mu_{\mathrm{Fe}}\, p_M \cos\,\theta$. All these quantities depend on the applied field and the temperature, which explains the complex behavior of the average magnetization shown in Fig. 3. At low temperature and in 5 T the measured average magnetization is $\overline{\mu}_{\mathrm{Fe}}=0.87$ and 0.45 μ_B/Fe atom for the 100 and 10 h ball-milled samples, respectively. The Mössbauer measurements yield $p_M=0.62$ and 0.41, cos $\theta=0.79$ and 0.63 for the two samples and the calculated moments are $\overline{\mu}_{\mathrm{Fe}}=1.78$ and 1.73 μ_B, respectively. These experimentally determined magnetic moment values support the conclusion drawn from the hf properties that the iron atoms in the grain boundaries have four iron nearest neighbors.

The most straightforward interpretation of our results is that ball-milling results in the formation of a magnetic shell around the nonmagnetic grain containing two adjacent iron layers. Obviously this shell is not neccessarily perfect, it can be somewhat disordered as the inner part of the grains, too. The coupling of the iron magnetic moments is ferromagnetic. The strong magnetic anisotropy [substantially stronger than that of α-Fe or Fe_3Al (Ref. 9)] directs the magnetic moments along the plane of the shell. In zero external magnetic field this arrangement forms no net magnetization. Since there is no preferred direction of the magnetization, it is very sensitive for small perturbations. It means that for increasing temperature the ferromagnetic ground state quickly disappears without a detectable transition temperature. On the other hand, even small magnetic fields can break this symmetry, causing the appearance of a net moment. The behavior of the system is ferromagnetic but saturation is not reached even in large fields because of the spherical distribution of the magnetic anisotropy directions.

The discussion and the coining of the term "magnetic foam" is credited to Professor A.S. Arrott. This work was supported by the Hungarian Research Fund (OTKA T31854).

[1] R. Skomski, J. Phys.: Condens. Matter **15**, R841 (2003).
[2] P. Grünberg, Phys. Today **54** (5), 31 (2001); Z. Q. Qiu, S. H. Mayer, C. J. Gutierrez, H. Tang, and J. C. Walker, Phys. Rev. Lett. **63**, 1649 (1989); U. Krey, J. Magn. Magn. Mater. **268**, 277 (2004).
[3] J. Balogh, L. Bujdosó, D. Kaptás, T. Kemény, I. Vincze, S. Szabó, and D. L. Beke, Phys. Rev. B **61**, 4109 (2000); J. Balogh, D. Kaptás, T. Kemény, I. Vincze, and G. Radnóczi, Phys. Rev. Lett. **82**, 4150 (1999).
[4] F. Elias, C. Flament, J.-C. Bacri, O. Cardoso, and F. Graner, Phys. Rev. E **56**, 3310 (1997); F. Graner, Y. Jiang, E. Janiaud, and C. Flament, *ibid.* **63**, 011402 (2000).
[5] O. Kubaschewski, *Iron-Binary Phase Diagrams* (Springer, Berlin, 1982), p. 5.
[6] R. D. Shull, H. Okamoto, and P. A. Beck, Solid State Commun. **20**, 863 (1976); W. Bao, S. Raymond, S. M. Shapiro, K. Motoya, B. Fåk, and R. W. Erwin, Phys. Rev. Lett. **82**, 4711 (1999); D. R. Noakes, A. S. Arrott, M. G. Belk, S. C. Deevi, Q. Z. Huang, J. W. Lynn, R. D. Shull, and D. Wu, *ibid.* **91**, 217201 (2003).
[7] H. Sato and A. Arrott, Phys. Rev. **114**, 1427 (1959).
[8] G. P. Huffman and R. M. Fisher, J. Appl. Phys. **38**, 735 (1967); Y. Yang, I. Baker, and P. Martin, Philos. Mag. B **79**, 449 (1999).
[9] S. Takahashi, X. G. Li, and A. Chiba, J. Phys.: Condens. Matter **8**, 11243 (1996); S. Takahashi, H. Onodera, X. G. Li, and S. Miura, *ibid.* **9**, 9235 (1997).
[10] T. M. Srinivasan, H. Claus, R. Viswanathan, P. A. Beck, and D. I. Bardos, *Phase Stability in Metals and Alloys*, edited by P. S. Rudman, J. Stringer, and R. I. Jaffee (McGraw-Hill, New York, 1967) p. 151; I. Vincze, Phys. Status Solidi A **7**, K43 (1971).
[11] S. J. Pickart and R. Nathans, Phys. Rev. **123**, 1163 (1961).
[12] R. Besson, A. Legris, and J. Morillo, Phys. Rev. B **64**, 174105 (2001).
[13] L. M. Di, P. I. Loeff, and H. Bakker, J. Less-Common Met. **168**, 183 (1991).
[14] T. Ungár and A. Borbély, Appl. Phys. Lett. **69**, 3173 (1996).
[15] I. Vincze, Nucl. Instrum. Methods Phys. Res. **199**, 247 (1982).
[16] G. P. Huffman, J. Appl. Phys. **42**, 1606 (1971); S. A. Makhlouf, M. Shiga, and K. Sumiyama, J. Phys. Soc. Jpn. **60**, 3537 (1991).
[17] M. B. Stearns, Phys. Rev. **147**, 439 (1966); I. Vincze and I. A. Campbell, J. Phys. F: Met. Phys. **3**, 647 (1973).
[18] B. Fultz and Z. Q. Gao, Nucl. Instrum. Methods Phys. Res. B **76**, 115 (1993).
[19] M. B. Stearns, Phys. Rev. **168**, 588 (1968).